ARVEDI ESP – REAL ENDLESS STRIP PRODUCTION: THE NEXT GENERATION OF PRODUCING HIGH-VALUE STEELS STARTED UP

A. Guindani, R.Venturini - Acciaieria Arvedi Spa, Cremona, Italy
A. Jungbauer, B. Linzer - Siemens VAI, Linz, Austria
S. Gelder, S. Bragin, C. Bernhard – Leoben University, Leoben, Austria

ABSTRACT

Thin slab casting and direct rolling has become a well established process in steelmaking with a worldwide installed annual capacity of more than 100 million tons. Acciaieria Arvedi SpA has operated a mini-mill for flat rolled products with a single strand ISP (In-line Strip Production) process since 1992. Since 2009, the new Arvedi ESP (Endless Strip Production) plant, a direct further development of the ISP process, has been successfully operating. The new process offers a high potential for the most economic production of thin hot strip down to 0.8 mm thickness of high quality steel grades, comprising high strength steels, such as HSLA, DP and Multi-Phase-Steels.
The present paper deals with the results of metallographic examinations on thin slabs and strip from low carbon HSLA-steel as well as the numerical simulation of the precipitation of NbC during hot rolling and subsequent cooling for S500MC-type steel grades. The results indicate the maximum utilization of the added micro-alloying elements, a key factor for the economic advantages of the ESP-technology over conventional steel production processes in producing HSLA-steel grades.

KEYWORDS

Thin slab casting and direct rolling, ESP, HSLA steel, microstructure evolution, precipitation kinetics, NbC-precipitation.

INTRODUCTION

Since 1992 Acciaieria Arvedi SpA has operated a mini-mill for flat rolled products with a single strand thin slab casting and rolling process using the ISP (In-line Strip Production) technology. Following this positive experience with its continuous thin slab casting and rolling process, improved in several stages over the years, the conclusion was to invest in a new ESP (Endless Strip Production) technology (**Fig. 1**), as a direct evolution of ISP [1]. Unique for both the ESP and ISP processes is the high reduction mill (HRM), which is directly connected to the high performance thin slab casting machine (in-line casting and rolling). The HRM results in a homogeneous microstructure before final hot rolling

Due to its highly compact lay-out with a total length of 190 m, lower investment costs are incurred for an Arvedi ESP line compared with conventional thin slab casting and direct rolling plants. Production costs are also noticeably lower than those of other thin slab plants and also of the ISP plant already operating in Cremona. Total energy consumption of the Arvedi ESP process is very low compared with that of a conventional casting and rolling process: depending on the final product, the energy consumption is 50-70% lower. Productivity of the ESP plant, based on a single

casting line, is about 2 mtpy for the first phase and a possible increase in mass flow from the caster may take capacity up to 3 mtpy.

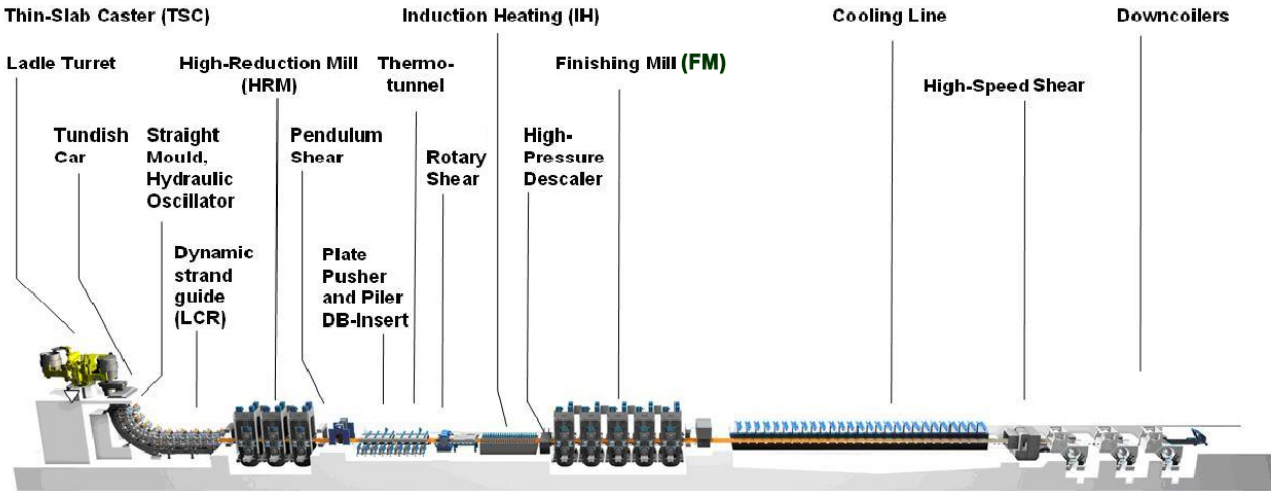

Fig. 1: Layout of the Arvedi ESP masterplant with main plant sections.

Due to endless rolling operations, the production of strip with uniform and repeatable mechanical properties is possible along the entire strip width and length and with the line's ability to produce ultra-thin hot rolled strip gauges of 0.8 mm, a subsequent cold rolling process will no longer be necessary for many strip applications.

Initial rolling at the HRM - directly connected to the caster without intermediate reheating - provides advantages in product geometry and material quality. After adjusting to the right temperature for end rolling using an inductive heater within the intermediate section, a 5-stand finishing mill allows optimal control of the behaviour of the steel strip during production. Furthermore, the two-step rolling concept enables the best possibilities for thermo-mechanical processing of strips through accurate temperature control along the line.

The first investigation of HSLA material produced at the ESP master plant in Cremona shows outstanding mechanical properties with a comparably low alloying content of the steel, which was observed in a similar manner at the Arvedi ISP line for numerous HSLA steel grades up to the strength class of S700. **Tab. 1** lists the possible production programme of an ESP line [2].

Tab. 1: Strip thickness range and steel grades for Arvedi ESP-plant [2].

Thickness	**0.80 – 12,7 mm**
Steel Grades	• Carbon steel (LC, ULC, Medium Carbon) • IF steel • HSLA • Pipe grades (up to API X80) • DP and Multi Phase Steel Grades • Silicon Steel (NGO, GO)

1. MICROSTRUCTURE EVOLUTION

Fig. 2 depicts a typical thermal history of a slab/strip in an ESP line. At the end of the casting machine, the surface temperature is between 1000 and 1100 °C, when assuming a casting speed of 6 m/min. Inside the thin slab the temperature is still 1300 °C. The stored thermal energy is required for the subsequent hot rolling process. The high temperature of the core ensures a low flow stress and thus lower conversion costs and an improved crown quality.
After reheating the intermediate strip to 1180°C in the induction unit, the strip is rolled to the final thickness in 5 finishing stands. A typical final strip temperature after hot rolling amounts to 850 °C. The cooling pattern is adjusted to the steel grade and the desired mechanical properties.

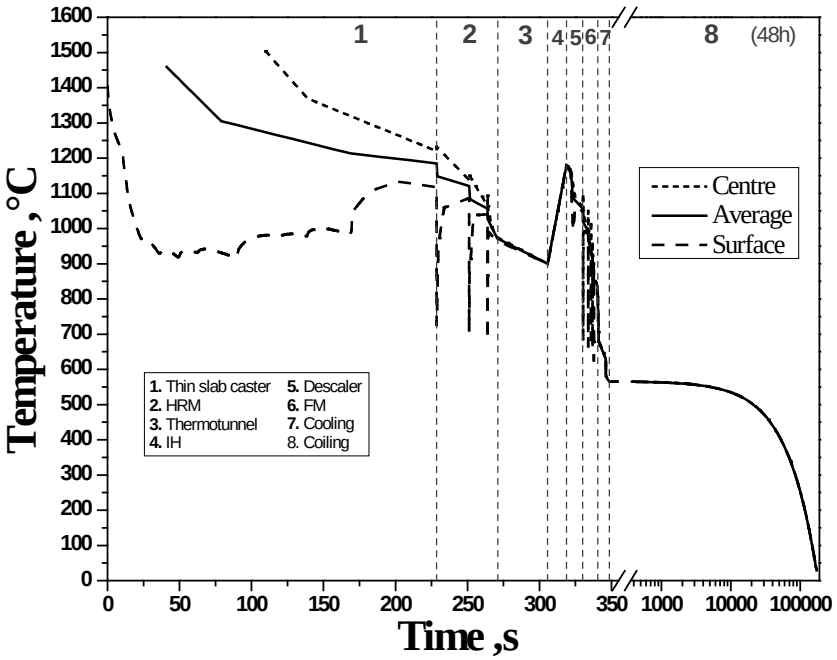

Fig. 2: Thermal history of the surface and the core of the thin slab and strip in an ESP line by casting speed 6m/min and thin slab thickness 80mm.

Fig. 3: Primary etching of a thin slab (0.06 wt.-% C, 80 mm thickness) from ESP Arvedi-masterplant.

Fig. 3 shows an example of the formation of the solidification microstructure in a thin slab (0.06 wt.-% C, 80 mm thickness). The primary structure, characterized for example by the primary dendrite arm spacing (PDAS), is fine compared with a slab of the same steel grade from a conventional continuous casting process. **Fig. 4** compares measured PDAS values from samples from the Arvedi ESP masterplant for a 0.06 wt.-% C steel grade and a 0.18 wt.-% C steel grade (80 mm thin slab). The typical order of magnitude of a PDAS at the surface amounts to 100 µm and to

300 µm near the centre of the thin slab. These values will serve as initial austenite grain size for austenite grain growth modelling.

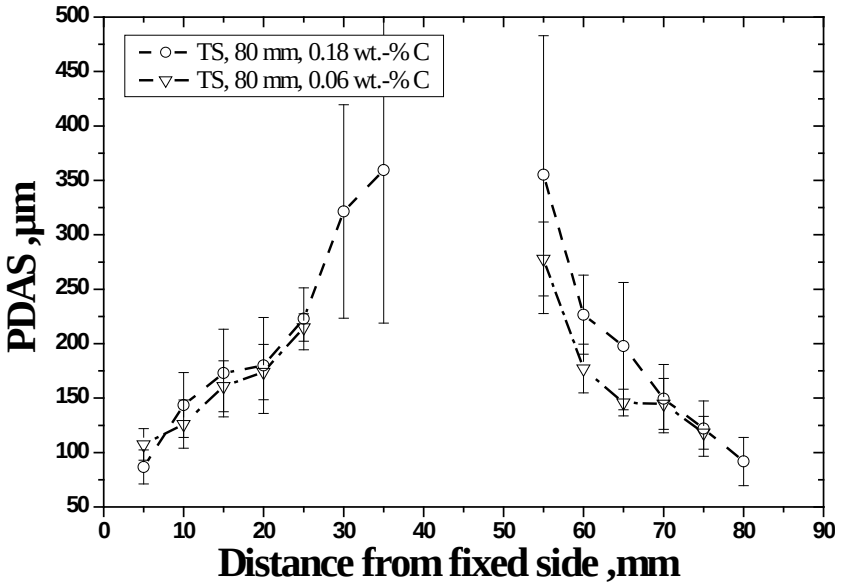

Fig. 4: PDAS for 0.06 and 0.18 wt.-% carbon steel, arithmetic mean and standard deviation.

1.1 AUSTENITE GRAIN GROWTH

The austenite grain size is an important parameter for the calculation of the precipitation of NbC in the rolling process. In order to predict the austenite grain size at the surface and the centre of the thin slab at the end of the casting machine, a recently published model was used [3]:

The following differential equation, proposed by Andersen and Grong [4], describes the variation in the average grain size with time (t) and temperature (T in K) in the presence of pinning precipitates:

$$\frac{d\,\bar{D}}{dt} = M_0^{*} \cdot e^{-\frac{Qapp}{R \cdot T}} \cdot \left(\frac{1}{\bar{D}} - \frac{1}{k} \cdot q_p \right)^{\left(\frac{1}{n}-1\right)} \qquad (1)$$

M_0^{*} denotes a kinetic constant ($4 \cdot 10^{-3}\ m^2 s^{-1}$). R is the gas constant (8.3145 J/molK) and n is the time exponent, set to 0.5. Q_{app} is the apparent activation energy for grain growth in J/mol and calculated by

$$Q_{app} = 167686 + 40562 \cdot (wt.-\%C) \qquad (2)$$

The driving force for grain growth is reciprocal to the actual grain diameter $\bar{D}$: Fine grains grow much faster compared to coarse grains and the grain growth is much higher at higher temperature. Due to the conditions of continuous casting machine, the grain growth rate will thus be the highest in - and immediately below - the mold and be counteracted by the pinning forces of precipitated particles (q_p). In the present case, the comparably high casting speed (and the related low residence

time in the casting machine) will suppress the precipitation of carbo-nitrides along grain boundaries. The last term of eq. 2 is thus neglected.

Fig. 5 shows the calculated austenite grain size at the surface, in the quarter-thickness position and in the centre of the thin slab versus time. The austenite grain growth starts with the δ/γ-transition temperature and therefore later in the centre. The initial grain size at the surface is 100 µm, 200 µm in the quarter-thickness position and 300 µm in the centre. At the end of the casting machine, the austenite grain diameter at the surface amounts to 600 µm and to 1700 µm in the centre.

The high thickness reduction and the high temperature of the thin slab core results in the recrystallization of the thin slab – almost independent from the initial austenite grain size. The austenite grain size after the 1st, 2nd and 3rd pass in the HRM was assumed to be 80, 50 and 40 µm. During the induction heating, the austenite grains grow again, and after respective rolling passes in the finishing mill the austenite grain size is 70, 50, 40, 20 and finally 15 µm. These assumptions correspond with published values from literature [5].

Temperature of γ/α-transition was calculated with the software IDS1.6. In addition grain size in the ferrite region is assumed as constant value 10 µm.

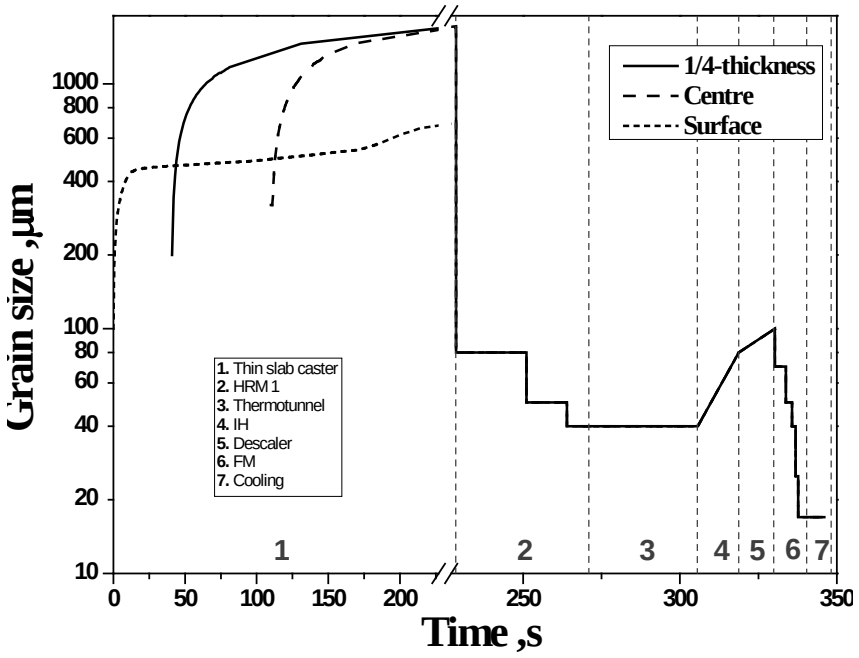

Fig. 5: Austenite grain growth in the casting machine and assumed values for the austenite grain size after recrystallization in the hot rolling mill and finishing mill.

1.2 DISLOCATION DENSITY

The evolution of dislocation density during deformation can be expressed as Eq.(3) [6]. This equation presents a relation between strain and dislocation density taking into account the increment of dislocation density at a given strain and the mechanism of dislocation annihilation in dynamic recovery.

$$\rho_d = \left(\frac{b\dot{\varepsilon}}{\varepsilon}\right)\left(1-\exp\left(\frac{-c\varepsilon}{\dot{\varepsilon}}\right)\right)+\rho_0 \tag{3}$$

The term b is a coefficient which represents an amount of an increasing rate of dislocation at a given strain and c is a coefficient for the description of the decrease rate of dislocations in dynamic recovery. ρ_0 is the initial dislocation density and is assumed to be 10^{12} m^{-1}.

$$b = b_{00}\exp(A\cdot Nb^{sol} + B\cdot Nb^{pre})\cdot D_\gamma^{\,m_b}\,\dot{\varepsilon}^{\,n_b}\exp\left(\frac{Q_b}{RT}\right) \tag{4}$$

$$c = c_{00}\exp(C\cdot Nb^{sol} + D\cdot Nb^{pre})\cdot D_\gamma^{\,m_c}\,\dot{\varepsilon}^{\,n_c}\exp\left(\frac{Q_c}{RT}\right) \tag{5}$$

Constants used in Eqs. (4) and (5) are given in **Tab. 2**. R is the gas constant (8.31J/mol/K). Additionally Nb^{sol} is the amount of solute Nb, while Nb^{pre} is the amount of precipitated Nb. D_γ corresponds to the austenite grain size.

Tab. 2: Constants for Eqs. (4),(5) [6]

b_{00}	1.33×10^{7}	mm^{-2}	n_b	0.105		D	0	$mass\%^{-1}$
A	0.92	$mass\%^{-1}$	Q_b	34100	$JK^{-1}mol^{-1}$	m_c	-0.182	
B	5.41	$mass\%^{-1}$	c_{00}	144	s^{-1}	n_c	1.02	
m_b	-0.207		C	-4.3	$mass\%^{-1}$	Q_c	18200	$JK^{-1}mol^{-1}$

In this work the Eq. (3) defines an increase of dislocation density during rolling, especially the contact time between roll and strip. The decrease in the dislocation density due to static recovery is expressed by Eq. (6) [7]. In this case the static recovery is caused by annihilation of dislocations at lattice defects like grain boundaries by climbing of dislocations after deformation in interpass time.

$$\rho_r = \left(\rho_d - \rho_0\right)\exp\left(-d\cdot t\right)+\rho_0 \tag{6}$$

The value of d is a coefficient representing the decrease rate of dislocations in static recovery.

$$d = d_0\exp(E\cdot Nb^{sol} + F\cdot Nb^{pre})\cdot D_\gamma^{\,m_d}\exp\left(\frac{-Q_d}{RT}\right) \tag{7}$$

Tab. 3: Constants for Eq. (7) [7]

d_0	1.05×10^{9}	s^{-1}
E	-85.6	$mass\%^{-1}$
m_d	-0.856	
Q_d	181500	$JK^{-1}mol^{-1}$

The decrease of dislocation density due to recrystallization was ignored.

2. MODELLING OF Nb(C,N)-PRECIPITATION

The nucleation kinetic of NbC, AlN and Cementite has been calculated, using the software package MatCalc (version 5.40 rel 1.000) [8,9], corresponding thermodynamic database "mc_steel" [10] and diffusion database "mc_sample_fe" [11]. The approach is based on the classical nucleation theory adopted for use in multi-component systems, it is giving the nucleation rate per unit volume and time as

$$J = N_0 \cdot \exp\left(\frac{-G^*}{k \cdot T}\right) \cdot \exp\left(\frac{-\tau}{t}\right) \qquad (8)$$

Above, N_0 denotes the total number of nucleation sites, k is the Boltzmann constant, T is the temperature and τ the incubation time. G* is the critical energy for nucleus formation. A detailed description of the calculation of these parameters can be found in [12]. In this model, dislocation induced accelerated precipitation is taken into account.

The precipitation of NbC has been calculated for ¼ thickness of strip. The steel grades are presented in **Tab. 4** and the rolling parameters in **Tab. 5**. Three selected steel grades have the same carbon, silicon and manganese content; the Al-content amounts to 0.038 wt.-% and the nitrogen content is 0.008 wt.-%. The Nb-content of these steel grades would be typical for the tensile strength classes of 355, 420 and 500 MPa.

Tab. 4: Steel composition for precipitation calculations.

Steel Grade	C, wt.-%	Mn, wt.-%	Si, wt.-%	Al, wt.-%	Nb, wt.-%
Nb15	0.05	0.5	0.2	0.038	0.015
Nb25	0.05	0.5	0.2	0.038	0.025
Nb42	0.05	0.5	0.2	0.038	0.042

Tab. 5: The rolling parameters for precipitation calculations.

	HRM1	HRM2	HRM3	FM1	FM2	FM3	FM4	FM5
Strain rate ,s^{-1}	1.1	2.4	4.1	14.1	33.5	83.9	85.2	70.3
Strain	0.5	0.425	0.4783	0.475	0.4444	0.4286	0.275	0.1724
Interval,s	22.5	12.857	66.238	3.5433	1.9651	1.125	0.8152	8.325

Possible nucleation sites for the NbC are grain boundaries and dislocations. The grain boundary density per unit volume results from the austenite grain growth calculations and assumptions. The dislocation density was calculated with the model presented in chapter 1.1. The described model was integrated directly in the software package MatCalc. **Fig. 6** shows the change of dislocation density during the process. The dislocation density is 10^{12} m^{-2} for the as-cast state, is jumping in each rolling pass and decreases during interpass time. The effect of Nb on the dislocation density is good visible. An increase in Nb is shown to enhance the final dislocation density.

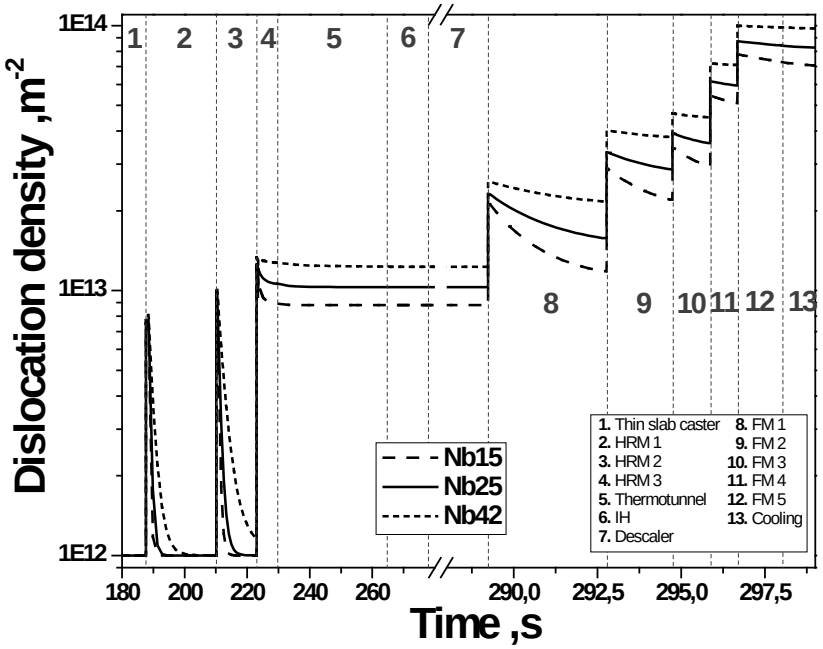

Fig. 6: Dislocation density in different positions along the ESP-line, assumed after [12,13].

3. MODELLING RESULTS

Fig. 7 depicts the number of NbC-precipitates versus time. The precipitation starts in the FM for the all steel grades. The first NbC precipitate in FM2, FM4 and FM5 by 0.042 wt.-% Nb, 0.025 wt.-% Nb and 0.015 wt.-% Nb respectively. Due to the fact that dislocation induced accelerated precipitation was included in the model, NbC precipitates exactly during deformation and by a negligible margin afterwards. In the interpass time occurs solely NbC coarsening, while number of precipitates remains almost constant.

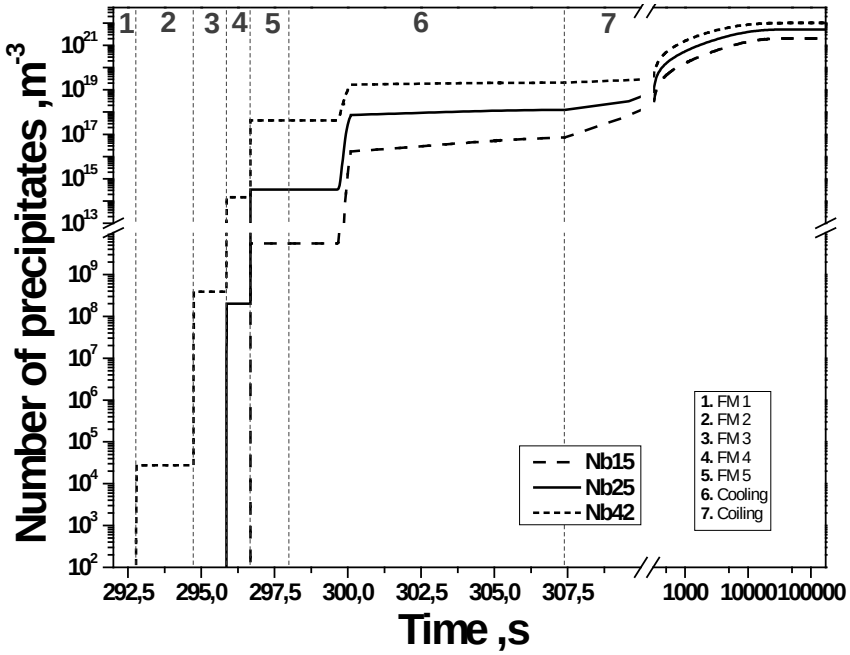

Fig. 7: NbC-precipitate density in $1/m^3$ for steel grades Nb15, Nb25 and Nb42 in Tab. 4 versus time.

At the end of the finishing mill, NbC reaches an approximate size of 34nm. During laminar cooling followed by coiling the nucleation rate becomes extremely high **Fig. 8**. It leads to the formation of a large amount of fine NbC. During this period, the major part of all NbC nucleate, which proves the very efficient usage of microalloying elements in the ESP process. Small NbC particles contribute mainly to the precipitation hardening and will increase the strength of the hot strip.

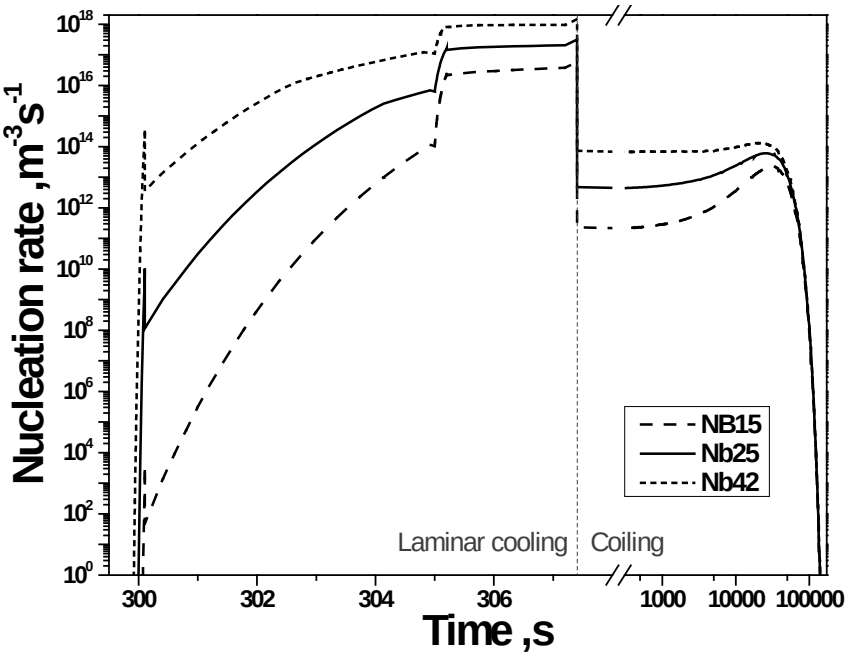

Fig. 8: NbC-nucleation rate in ferrite in $1/m^3s^1$ for steel grades 1, 2 and 3 in Tab. 2 versus time.

Fig. 9 shows – in correspondence with the results in figure 7 - the phase fraction of NbC, relatively the maximum value of NbC by equilibrium, versus time. For steel grade Nb15 the NbC phase fraction amounts to 0,74%, for steel Nb25 it amounts to 2,36%. The final NbC-phase fraction of steel Nb42 is 7,19%. It is clearly visible from these results that an increasing Nb-content results in an increasing number, nucleation rate and phase fraction of precipitates and – thus – in an increasing tensile strength.

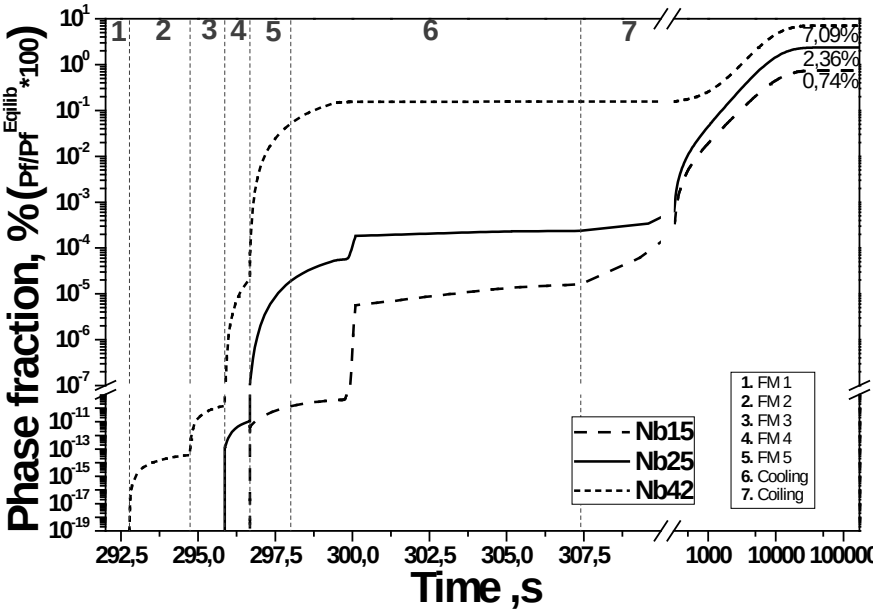

Fig. 9: NbC-phase fraction for steel grades Nb15, Nb25 and Nb42 in Tab. 2 versus time.

As has already been outlined before, the solidification structure of the thin slab is very fine and comparable with the near surface area of a conventional cast slab. Even under the conditions of the conventional casting process, primary interdendritic NbC-precipitates form mainly in the segregated centre region [13,14]. The fine columnar solidification structure of the thin slab prevents the precipitation of coarse carbo-nitrides during solidification. By all considered amount of Nb, the whole amount of Niobium is available for precipitation in the finishing mill and during the subsequent cooling of the strip. The efficiency of Niobium as micro-alloying element is thus markedly higher compared with the conventional production process.

4. RESULTS FROM PLANT TRIALS

Tab. 6 sums up first published results from plant trials as the Arvedi ESP plant in Cremona [2]. For both Nb – microalloyed steels, the strength is higher compared with conventionally produced steel strip of the same composition and the elongation meets the expectations.

Tab. 6: The rolling parameters for precipitation calculations.

	Rm	**ReH**	**A_{80}**	**%C**	**%Mn**	**%Nb**
S235JR	410	330	31	0,04	0,20	-
S355MC	440	375	30	0,05	0,20	0,020
S420MC	470	430	28	0,05	0,50	0,025

In HSLA steel grades, in spite of the low level of Nb, fine precipitates were observed in the matrix, with a size range of 20-40 nm (**Fig. 10**). These fine particles, which make the major contribution to dispersion strengthening, are NbC, which mainly precipitate during cooling at the run out table after the finishing mill, proving the very efficient use of microalloying elements of ESP process.

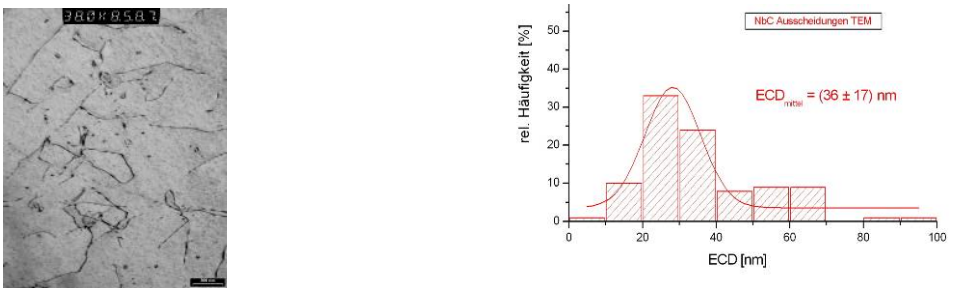

Fig. 10 : TEM picture of of NbC precipitations and statistical evaluation of diameters.

5. CONCLUSIONS

The present paper focuses on research on the production of HSLA-steel strip under the conditions of the Arvedi ESP plant in Cremona.

- The metallographic examinations on the cast thin slabs with a thickness of 80 mm prove that both the solidification microstructure and grain size are fine compared with the conventional slab casting process.
- The metallographic examination and mechanical testing of the hot rolled strip points at the fine and homogeneous ferrite microstructure and a high yield strength.

- The precipitation of NbC has been modeled by use of the software package MatCalc.
- The results show that NbC precipitates mainly during the final rolling passes in the finishing mill.
- Even though the precipitates are fine, the phase fraction of the precipitates is high underlining the high efficiency of the added microalloying elements in the Arvedi ESP process.

Future work will focus on the influence of changing production parameters for the same steel grades in the precipitation model (e.g. casting speed and temperature after inductive heating).

REFERENCES

1) G. ARVEDI, F. MAZZOLARI, J. SIEGL, G. HOLLEIS and A. ANGERBAUER, Proc. Rolling & Processing Conference 08, Linz, Austria (2008).
2) A. GUINDANI, R. VENTURINI and B. LINZER, Technical Summit on Arvedi ESP Technology, Cremona, Italy (2010).
3) C. BERNHARD, J. REITER and H. PRESSLINGER, Met. Trans. 39B (2008), p. 885
4) I. ANDERSON and O. GRONG, Acta metal. Mater. 43 (1995), p. 2673
5) C.A. MUOJEKWU, D.Q. JIN, V. HERNANDEZ, I.V. SAMARASEKERA and J.K. BRIMACOMBE, Proc. 38th Mech. Working Steel Proc. Conf., Cleveland, Ohio, USA (1996).
6) A. YOSHIE, T. FUJITA, M. FUJIOKA, K. OKAMOTO and H. MORIKAWA, ISIJ 36 (1996), p. 467.
7) A. YOSHIE, T. FUJITA, M. FUJIOKA, K. OKAMOTO and H. MORIKAWA, ISIJ 36 (1996), p. 474.
8) J. SVOBODA, F.D. FISCHER, P. FRATZL and E. KOZESCHNIK, Mater.Sci.Eng. A385 (2004) 166-74
9) E. KOZESCHNIK J. SVOBODA, P. FRATZL and F.D. FISCHER, Mater.Sci.Eng. A385 (2004) 157-65
10) Institute of Materials Science and Technology, Vienna University of Technology 2009 Thermodynamic Database “mc_steel” MatCalc, version 1.91
11) Institute of Materials Science and Technology, Vienna University of Technology 2010 Diffusion Database “mc_steel” MatCalc, version 1.04
12) R. RADIS and E. KOZESCHNIK, Modelling Simul. Mater. Sci. Eng. 18 (2010), p. 1.
13) H. PRESSLINGER, M. MAYR, E. TRAGL and C. BERNHARD, steel research int. 77 (2006), p. 107.
14) H. PRESSLINGER, S. ILIE, A. SCHIEFERMÜLLER, A. PISSENBERGER, E. PARTEDER and C. BERNHARD, ISIJ 46 (2006), p. 1845.